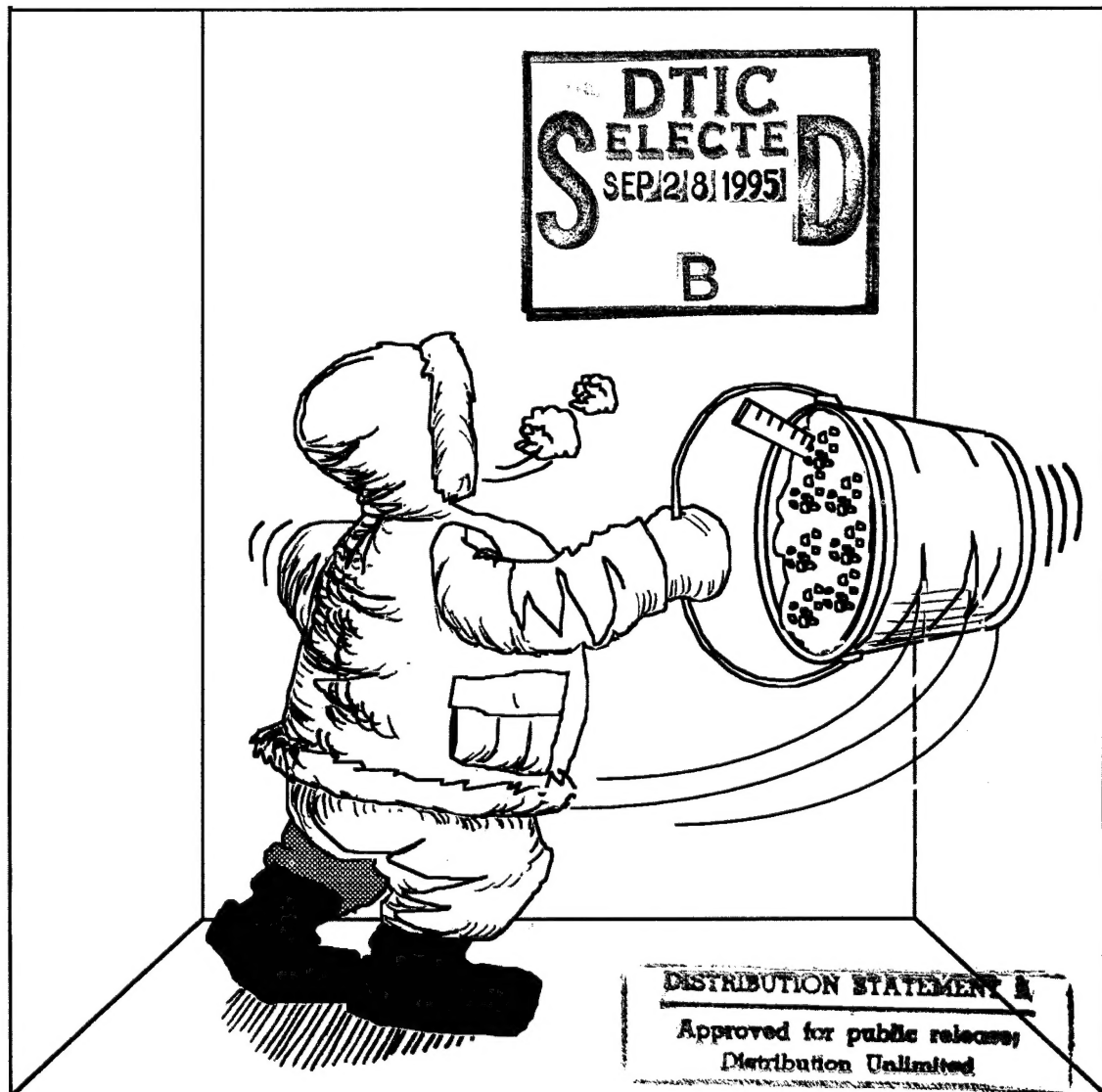




# Initial Results From Small-Scale Frost Heave Experiments in a Centrifuge

Stephen A. Ketcham and Patrick B. Black

May 1995



19950926 086

DTIC QUALITY INSPECTED 5

***Abstract***

Frost heave modeling is presented as a problem of small-scale experimental modeling. Scale factors applicable to frost heave model testing are reviewed, and initial data from frost heave experiments conducted as centrifuge model tests are presented. Ongoing improvements, modifications and future model tests are discussed.

CRREL Report 95-9



**US Army Corps  
of Engineers**

Cold Regions Research &  
Engineering Laboratory

# **Initial Results From Small-Scale Frost Heave Experiments in a Centrifuge**

Stephen A. Ketcham and Patrick B. Black

May 1995

Prepared for  
OFFICE OF THE CHIEF OF ENGINEERS

Approved for public release; distribution is unlimited.

DTIC QUALITY INSPECTED 5

## PREFACE

This report was prepared by Stephen A. Ketcham, Research Civil Engineer, Civil and Geotechnical Engineering Research Division, and Patrick B. Black, Research Physical Chemist, Applied Research Division, Research and Engineering Directorate, U.S. Army Cold Regions Research and Engineering Laboratory, Hanover, New Hampshire.

Funding for this work was provided by the CRREL In-House Laboratory Independent Research program and by the Office of the Chief of Engineers under DA Project 4A762784AT42, *Design, Construction and Operations Technology for Cold Regions*, Task CA, Work Unit D02, *Investigation and Design of Foundations in Cold Regions*.

The authors thank Edwin Chamberlain and Sally Shoop for their technical reviews of this report. They also thank James Morse, who provided valuable suggestions for the heater design of the frost heave cell.

The contents of this report are not to be used for advertising or promotional purposes. Citation of brand names does not constitute an official endorsement or approval of the use of such commercial products.

## CONTENTS

|   | Page |
|---|------|
| Preface .....   | ii   |
| Introduction .....  | 1    |
| Centrifuge modeling background .....                                      | 1    |
| Frost heaving modeling .....  | 3    |
| Experimental technique .....  | 3    |
| Results .....   | 5    |
| Conclusions and future experiments .....                                  | 7    |
| Literature cited .....  | 8    |
| Appendix A: Some scale factors for conventional centrifuge modeling ..... | 11   |
| Appendix B: Scaling the Rigidice model .....                              | 15   |
| Abstract .....  | 19   |

## ILLUSTRATIONS

### Figure

|   |   |
|---|---|
| 1. Frost heave scenarios .....  | 1 |
| 2. Sample containers and sample preloading equipment .....            | 4 |
| 3. Sample containers in the centrifuge .....                          | 4 |
| 4. Sample used in the 8-g experiment .....                            | 5 |
| 5. Sample used in 32-g experiment .....                               | 6 |
| 6. Design of a simple frost heave cell for the small centrifuge ..... | 7 |

## TABLES

### Table

|  |   |
|--|---|
| 1. Scale factors for geotechnical centrifuge modeling .....  | 2 |
| 2. Centrifuge test conditions along with measured model and<br>calculated prototype results for New Hampshire silt ..... | 6 |

|                    |                                     |
|--------------------|-------------------------------------|
| Accession For      |                                     |
| NTIS GRA&I         | <input checked="" type="checkbox"/> |
| DTIC TAB           | <input type="checkbox"/>            |
| Unannounced        | <input type="checkbox"/>            |
| Justification      |                                     |
| By _____           |                                     |
| Distribution/_____ |                                     |
| Availability Codes |                                     |
| Dist               | Avail and/or<br>Special             |
| A-1                |                                     |

# Initial Results From Small-Scale Frost Heave Experiments in a Centrifuge

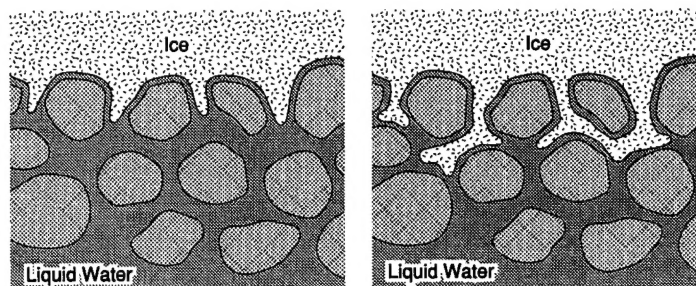
STEPHEN A. KETCHAM AND PATRICK B. BLACK

## INTRODUCTION

Frost heave is the displacement of soil caused by the formation of segregated ice lenses in a freezing soil body. Although the process is complicated, a number of researchers have developed models to describe and analyze the mechanics of frost heave [see Kay and Perfect (1988) and Nakano (1990) for recent reviews]. One of these is Miller's (1978, 1980a) "Rigidice model."

In the Rigidice model the soil body is divided into three regions. The first region comprises already-frozen soil that might contain relic ice lenses but definitely contains a growing ice lens. The second region, which contains a growing ice lens at one end and unfrozen soil at the other, is called the frozen fringe (Miller 1978, 1980b). The third comprises unfrozen soil and is the source of mass and energy for the heaving process. Miller (1978, 1980b) calls this three-region frost heave scenario "secondary heave." In a variation of secondary heave, which Miller designates "primary heave," there is no frozen fringe but rather an abrupt boundary between the growing ice lens and the unfrozen soil. Figure 1 illustrates primary and secondary heaving conditions.

Miller presented a mathematical description of the Rigidice model in 1978. He followed with finite-element (O'Neill and Miller 1985) and finite-difference implementations (Black and Miller 1985), comparisons to experimental data (Black and Miller 1985) and a scaling analysis of the governing equations of the model (Black 1985, Miller 1990). Of particular interest for this paper is Miller's scaling analysis. This analysis and the distinct role of gravitational body force in the heaving process led Miller to conclude that scale mod-



a. Primary heave.

b. Secondary heave.

Figure 1. Frost heave scenarios.

eling of frost heave would best be conducted as a body force analog and that a small-scale frost heave test conducted in a centrifuge would be appropriate for this purpose.

An objective of our ongoing work is to experimentally confirm Miller's conclusion and the scale factors inherent in his scaling analysis. This report presents a brief overview of frost heave centrifuge modeling from two perspectives: conventional geotechnical centrifuge modeling and scaling of the differential equations of the Rigidice model. We describe two initial model experiments in which silt specimens were partially frozen in 8-g and 32-g centrifugal fields. The experiments were performed to provide a basis for equipment development and further experiments. Plans for the equipment and future tests are presented as well.

## CENTRIFUGE MODELING BACKGROUND

Physical modeling is the testing of a small-scale model so that the response of a prototype can be inferred from the model response. A model is

**Table 1. Scale factors for geotechnical centrifuge modeling. (After Scott and Morgan 1977, Croce et al. 1985, Savidou 1988.)**

| Quantity                             | Prototype | Model            |
|--------------------------------------|-----------|------------------|
| Linear dimension and displacement    | 1         | 1/N              |
| Area                                 | 1         | 1/N <sup>2</sup> |
| Volume                               | 1         | 1/N <sup>3</sup> |
| Mass density                         | 1         | 1                |
| Mass                                 | 1         | 1/N <sup>3</sup> |
| Acceleration                         | 1         | N                |
| Stress                               | 1         | 1                |
| Force                                | 1         | 1/N <sup>2</sup> |
| Strain                               | 1         | 1                |
| Energy density                       | 1         | 1                |
| Energy                               | 1         | 1/N <sup>3</sup> |
| Temperature                          | 1         | 1                |
| Time (for viscous force similarity)  | 1         | 1                |
| Time (for inertial force similarity) | 1         | 1/N              |
| Time (for seepage force similarity)  | 1         | 1/N <sup>2</sup> |

said to be similar to the prototype when each significant engineering variable of the model is related by a proportionality or scale factor to the corresponding variable of the prototype. Scale factors are governed by the physics and model laws of the problem. They are used to design the model and to interpret the measured model response as the prototype response.

Physical models of civil engineering structures are often designed so that the model will be geometrically similar to the prototype, so that significant forces in the model are proportional to the forces in the prototype, and so that the model's response to loads will be kinematically similar to that of the prototype. Geometric similarity means that all parts of the model have the same shapes as the corresponding parts of the prototype, and kinematic similarity means that the motions of the model are similar to the motions of the prototype at corresponding times. When all net forces are proportional, dynamic similarity is said to exist (Langhaar 1951). In general, the mechanical response of a structural model to forces is observed and interpreted as the prototype response.

Centrifuge modeling is a physical modeling technique in which the weight stresses of a structure are simulated by the placement of a small-scale model in a centrifugal field. This technique is of proven benefit for modeling soil structures, because the form and magnitude of the soil response are often greatly dependent on weight-generated effective stresses and because the loading can be dominated by weight loads. As described in Appendix A, when the prototype soil

is used in the model, model laws of soil mechanics, together with requirements for geometric and kinematic similarity, lead to scale factors for centrifuge modeling. Several are shown in Table 1 as ratios of the model quantity to the prototype quantity for a model that is 1/N the size of the prototype. Following Croce et al. (1985), a number of these are derived in Appendix A.

Many of the scale factors listed in Table 1 are basic structural modeling scale factors and can be derived from the mechanical considerations (Langhaar 1951). The scale factor for acceleration, which is  $N$ , can be derived from the consideration that weight forces should be scaled as other forces, and it implies the need for an increased gravity field (Croce et al. 1985). The centrifuge is used to approximate this condition by subjecting a model to the constant angular velocity  $\Omega$  according to

$$\Omega = \sqrt{\frac{Ng}{r}} \quad (1)$$

where  $g$  = acceleration due to Earth's gravity  
 $r$  = representative radius of the model from the axis of rotation  
 $r\Omega^2$  = radial acceleration of the model at this radius.

In this context,  $N$  can be considered as a nominal gravity level:

$$N = \frac{r\Omega^2}{g} \quad (2)$$

and the model can be considered to be subjected to an inertial field equivalent to  $N$  gravities, or  $Ng$ . As described by Langhaar (1951), if self-weight stresses have a negligible influence on the prototype response, or if partial dynamic similarity is acceptable to the modeler, the principles discussed here for centrifuge modeling and the scaling relations of Table 1 can be applied to models tested at 1  $g$ . However, because self-weight stresses typically cannot be neglected for geotechnical prototypes, centrifuge modeling has become a conventional technique.

As indicated in Table 1, there are different time scales for the forces of viscous, inertial and seepage phenomena. As a result, time scale conflicts can occur for certain modeling problems, and dynamic similarity can be impossible to achieve. Thus the experimenter must consider the limitations imposed by the model laws and scale factors when designing a model experiment. Appendix A presents derivations of these time scales.



The use of prototype soils in centrifuge models is an accepted practice and is an attempt to achieve structural response similarity of the model and prototype by ensuring that the constitutive response of the model will be as close as possible to the prototype material response. Langhaar (1951) and Schmidt and Holsapple (1980) have suggested that when a model is made of the material of the prototype, when there are no time scale conflicts, and when the material response is independent of model size, prototypes with general constitutive behavior such as nonlinear elasticity, plasticity and fracture can be modeled by following the scaling relations of Table 1. The use of prototype soils within typical scale models (e.g., 1/25 to 1/100 scale) does not generally result in scale effects unless soils with particles larger than sands are tested. It is common in centrifuge testing to ensure that the parts of models are much larger than the soil particle sizes so that particle size does not result in adverse scale effects. It is also common to test different scale models of the same prototype to ensure that scale effects are insignificant.

To correctly model heat transfer processes in saturated ground, the model and prototype must be thermally similar, in addition to being geometrically, kinematically and dynamically similar. Thermal similarity includes the similarity of internal energy and energy density, as evidenced by similar temperature changes and differences at homologous points. For centrifuge modeling, Savidou (1988) has shown that the scale factor for temperature change is 1 and that the time scale factor for conductive and convective heat transfer through a soil body is  $1/N^2$ , which is the same as the time scale factor for seepage processes.

## FROST HEAVE MODELING

When the differential equations of a particular mechanical problem or physical process are known to the modeler, a scaling analysis can be performed to determine techniques for appropriate small-scale modeling of the problem. Scaling is a method of dissolving passive physical parameters into active variables in a differential equation (Miller 1980a). Any solution to the scaled equation is also a solution to any other distinct physical system that can obtain the same scaled variables and scaled boundary conditions from its distinct physical parameters. The earliest scaling analysis of soils containing water and its vapor

was conducted by Miller and Miller (1956). They presented a set of scaled relationships describing the isothermal flow of liquids in the unsaturated soil, and they concluded from length, stress and time scale factors that a centrifuge experiment would be appropriate for small-scale modeling of this flow (Miller and Miller 1955). Miller's 1990 scaling analysis of the Rigidice equations was an extension of these earlier investigations of scaling laws for unsaturated porous flow. An expansion of this analysis is presented in Appendix B.

Like the previous scaling investigations, Miller's Rigidice analysis was based on scaling the effects of surface tension and viscous flow, but it also incorporated heat transfer, phase change of the pore water, and ice lens initiation and growth. The analysis yielded reduced equations that are consistent with the techniques of conventional centrifuge modeling and the scale factors in Table 1. It provided a complete theoretical basis for small-scale frost heave modeling in a geotechnical centrifuge. Miller (1990) emphasized that the ratio of model time to prototype time for the freezing process in a centrifuge model would be  $1/N^2$ , and he cited Pokrovsky and Fyodorov (1969) as the first to suggest the use of a geotechnical centrifuge for modeling frozen and freezing ground structures. On the basis of Miller's earlier unpublished discussions on model laws for soil freezing, Black (1985) presented a set of scaling relationships for frost heave centrifuge modeling, recommended a simple model study of frost penetration and heave, and demonstrated that a great time savings would be obtained over a full-scale experiment.

## EXPERIMENTAL TECHNIQUE

Our preliminary soil freezing experiments were conducted on an International Equipment Company Model PR-2 centrifuge. The device is a small refrigerated centrifuge manufactured for applications in biology, bacteriology, physiology and biochemistry. It has a nominal operating radius of 0.2 m for the rotor and cups used in our test configuration. During the experiments the centrifuge was located in a coldroom with an ambient temperature of approximately 4.5°C.

Two insulated sample containers were made to allow simultaneous testing of saturated soil samples. In each container a Plexiglas cylinder enclosed the soil sample. The cylinder was mount-



ed on a porous plastic base to allow water flow to the sample from an exterior annular reservoir. Except for the upper end of the Plexiglas cylinder, the cylinder and reservoir were surrounded by insulation. The upper end of the cylinder was left open to the air. The insulated sample containers were made to fit into cylindrical cups that were supplied with the centrifuge. These cups have inside dimensions of 98 mm in diameter and 120 mm in height.

The test samples comprised a saturated New Hampshire silt compacted in the Plexiglas cylinder

der of the assembled sample container. The nominal sample dimensions were 10 mm in height and 34 mm in diameter. We prepared each sample at room temperature by mixing 12.5 g of the New Hampshire silt with water to form a slurry with an 80% water content. The slurry was poured into the Plexiglas cylinder, preloaded and consolidated with a vertical stress of 14.1 kPa. Free water expelled at the sample surface was removed. The dry mass density of the consolidated samples was approximately  $2040 \text{ kg/m}^3$ . The sample containers and sample preloading equipment are shown in Figure 2.

Following the sample preparation, the insulated sample containers were taken to the coldroom, placed in the centrifuge cups, and immediately tested. Figure 3 shows the sample containers in the centrifuge. The radius from the centrifuge axis to the sample bottom was 0.196 m. To achieve nominal gravity levels of 8 and 32 g at desired reference radii in the tests (Cooke 1991), the centrifuge was operated at rotational velocities close to 193 and 387 rpm, respectively. The effect of Earth's gravity on the equilibrium orientation of the centrifuge cups was considered in our calculation of these velocities. The experiments were conducted with minimal control of the temperature of the sample and with minimal measurement of the sample response. Our hope for these preliminary experiments was simply that we could freeze the samples from the top down. We operated the centrifuge with the centrifuge chamber closed to the coldroom atmosphere, and we maintained the chamber temperature close to our desired temperature of  $-2^\circ\text{C}$  by manually turning on and off the refrigeration system of the

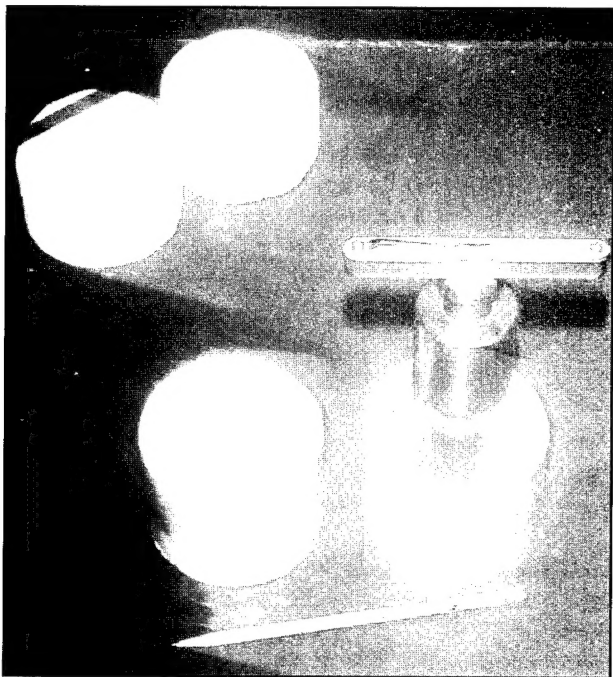


Figure 2. Sample containers and sample preloading equipment.



Figure 3. Sample containers in the centrifuge.

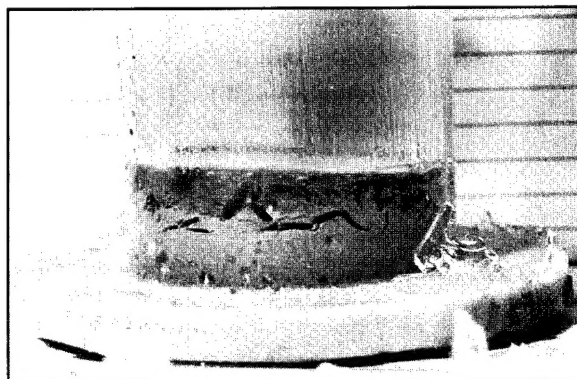
centrifuge. Manual operation was necessary because of the crude response of the centrifuge's refrigeration control system. The duration of the experiments was approximately five hours. A thermocouple located at the top of the closed centrifuge chamber provided the only temperature measurement for the tests. There was no measurement of the temperature of the sample. In addition there was no measurement of the sample heave as a function of time.

## RESULTS

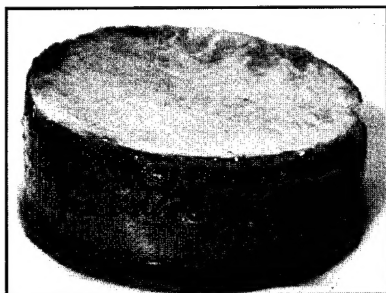
The experimental data consist of measurements of the temperature in the centrifuge chamber, measurements of the height of the samples at the beginning and end of the tests, and observations and photographs of the samples following the tests. Table 2 presents the measurements for the

8-g and 32-g tests along with the corresponding 1-g prototype values calculated using either the Table 1 scale factors or the scaling process described in Appendix B. The temperature records reveal that the chamber temperature varied by  $\pm 0.25^{\circ}\text{C}$  from the desired temperature of  $-2^{\circ}\text{C}$ . Figures 4 and 5 show the 8-g and 32-g samples, respectively, before and after their extrusion from the cylinder and after crudely cutting them to examine the interior ice lens configuration. The air temperature surrounding the samples during cutting was  $4.5^{\circ}\text{C}$ . As a result the figures show the samples in progressive stages of melting.

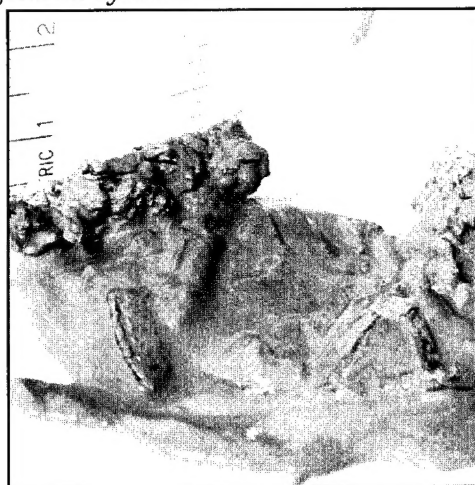
In the five-hour test period, only the upper 5–8 mm of the 8-g and 32-g samples froze. This was a desired result, as it confirms that the freezing occurred from the top down. This was important since we had no other means of monitoring the progress of the freezing front. That the 8-g and 32-g samples would freeze to about the same depth



*a. Prior to extrusion from the cylinder.*



*b. After extrusion from the cylinder.*



*c. After cutting to examine the interior ice lens configuration.*

*Figure 4. Sample used in the 8-g experiment.*

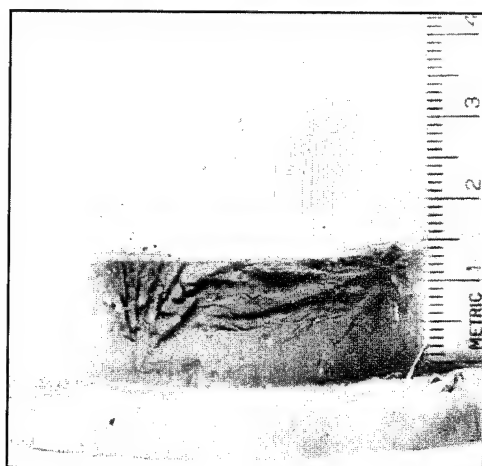
**Table 2. Centrifuge test conditions along with measured model and calculated prototype results for New Hampshire silt.**

| Quantity                              | <i>1/8-scale experiment</i> |                  | <i>1/32-scale experiment</i> |                  |
|---------------------------------------|-----------------------------|------------------|------------------------------|------------------|
|                                       | <i>Model</i>                | <i>Prototype</i> | <i>Model</i>                 | <i>Prototype</i> |
| Acceleration (g)                      | 8                           | 1                | 32                           | 1                |
| Dry bulk density (kg/m <sup>3</sup> ) | 2040                        | 2040             | 2040                         | 2040             |
| Sample height (mm)                    | 10                          | 80*              | 10                           | 320*             |
| Sample diameter (mm)                  | 34                          | 272*             | 34                           | 1088*            |
| Upper surface temperature (°C)        | -2                          | -2 <sup>†</sup>  | -2                           | -2 <sup>†</sup>  |
| Duration of test (hr)                 | 5                           | 320**            | 5                            | 5120**           |
| Frost penetration (mm)                | 5-8                         | 40-64*           | 5-8                          | 160-256*         |
| Heave (mm)                            | 1-2                         | 8-16*            | 3                            | 96*              |

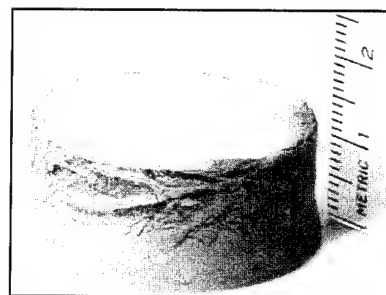
\*Table 1 or eq B18

<sup>†</sup>Table 1 or eq B10

\*\*Table 1 or eq B24 with B18



*a. Prior to extrusion from the cylinder.*



*b. After extrusion from the cylinder.*



*c. After cutting to examine the interior ice lens configuration.*

*Figure 5. Sample used in 32-g experiment.*

was also an expected result, since an inertial field should not directly affect the heat transfer. From the sample height measurements we estimated the average heave of each of the two 8-g samples to be approximately 1–2 mm and the average heave of each of the two 32-g samples to be approximately 3 mm.

The 8-g test samples froze under a stress field that is approximately similar to the stress field of an 8-cm column of soil at 1 g, and the 32-g test samples froze under a stress field approximately similar to a 32-cm column of soil at 1 g. The differences in the configurations of the interior lenses of the 8-g samples and the 32-g samples were the most interesting result of the experiments. In the 8-g samples the ice lenses did not form in distinct horizontal layers. The ice clearly formed thin ( $< 0.5$  mm) lenses that separated the soil particles, but the lenses appeared randomly oriented. In the 32-g samples, however, a horizontal bias to the lens orientation was evident. These observations are consistent with an explanation that might be used for similar observations in the upper 4 cm and the upper 16 cm of a silt column in 1-g freezing tests: that a randomly oriented lens configuration can develop in shallow soils that do not have a significant vertical overburden stress, and a horizontally oriented lens pattern can develop in deeper soils that have a greater overburden stress.

The results of the experiments are crude, yet they provide two pieces of information for the design of equipment for further experiments. First, the indication that the freezing occurred from the top down in the samples suggests that we can proceed with a one-dimensional cylindrical sample configuration in our small centrifuge tests, and second, the apparent consistency of the lens configurations of the 8-g and 32-g samples with corresponding prototype behavior suggests that with control of the experiments the applicability of the centrifuge for frost heave modeling can be investigated.

## CONCLUSIONS AND FUTURE EXPERIMENTS

A design of a simple frost heave cell for the small centrifuge is illustrated schematically in Figure 6. The cell will be instrumented with lower and upper heaters and with temperature and displacement measurement sensors. The lower heater will be a thin heating pad mounted onto the bottom of the centrifuge cup, and the upper heater will be a cartridge heater mounted in a radial-fin heat sink. A fan will be installed above the heater to circulate air past the heat sink fins to the upper sample surface. The upper heater will not be

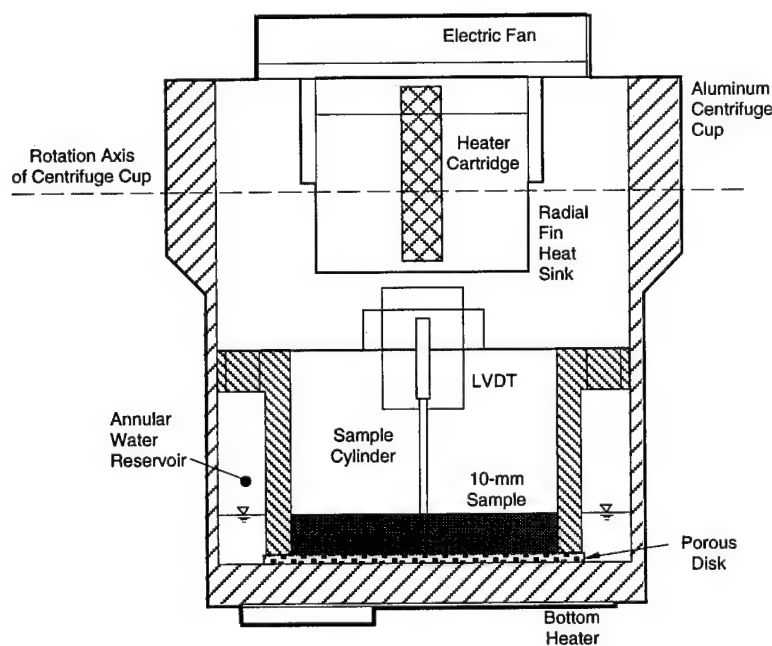


Figure 6. Design of a simple frost heave cell for the small centrifuge. The diagram shows the cross section of the inside of the centrifuge chamber during operation; the centrifuge rotor arm is not shown.

in contact with the sample and thus will not load the sample. Both heaters will be controlled using feedback controllers. An electrical slip ring assembly will be installed on the centrifuge axis to allow power and instrumentation signals to be passed to and from the cell while the centrifuge is operating. The centrifuge will be operated in a coldroom at a temperature below freezing (e.g.,  $-5^{\circ}\text{C}$ ), and the heaters will be controlled to maintain upper and lower sample surfaces at desired temperatures. Thin sectioning and image analyzing techniques will be used to examine the lens ice distribution, orientation and thickness.

The modeling at different scales or acceleration fields will be used to examine the validity of our frost heave modeling. Specifically a series of different scale models of the same prototype will be tested, and the model displacement vs. time records will be interpreted to see if each of the prototype heave vs. time predictions are essentially the same. If the one-dimensional heave process can be modeled, then other tests will be conducted regarding heave forces and the interaction of heaving soil with foundation and other structural members.

Additional analysis will compare experimental measurements to predictions using a recent version of the Rigidice model (Black 1994). While the exact location and thickness of individual ice lenses in the model and prototype will most likely not be predictable, the total amount of heave, penetration and fluxes should. This will be the topic of future discussions.

## LITERATURE CITED

- Black, P.B.** (1985) The RIGIDICE model of frost heave and its input functions. Ph.D. Thesis, Cornell University.
- Black, P.B.** (1992) Soil water: liquid, vapor and ice. *Encyclopedia of Earth System Science*, 4: 259–269.
- Black, P.B.** (1994) Heave 4.0, A finite difference implementation of the RIGIDICE model. Unpublished.
- Black, P.B. and Miller, R.D.** (1985) A continuum approach to modeling frost heaving. *Freezing and Thawing of Soil Water Systems* (D.M. Anderson and P.J. Williams, Ed.). American Society of Civil Engineers, Technical Council on Cold Regions Engineering, p. 36–45.
- Cooke, B.** (1991) Selection of operative centrifuge radius to minimize stress error in calculations. *Canadian Geotechnical Journal*, 28: 160–161.
- Croce, P., V. Pane, D. Znidarcic, H.-Y. Ko, H.W. Olsen and R.L. Schiffman** (1985) Evaluation of consolidation theories by centrifuge modelling. *Application of Centrifuge Modelling to Geotechnical Design*, p. 381–401 (W.H. Craig, Ed.). Rotterdam: Balkema.
- Kay, B.D. and E. Perfect** (1988) State of the art: Heat and mass transfer in freezing soils. *Ground Freezing 88, Proceedings of the Fifth International Symposium on Ground Freezing* (R.H. Jones and J.T. Holden, Ed.). Rotterdam: Balkema.
- Langhaar, H.L.** (1951) *Dimensional Analysis and Theory of Models*. New York: John Wiley and Son.
- Loch, J.P.G.** (1978) Thermodynamic equilibrium between ice and water in porous media. *Soil Science*, 126(2): 77–80.
- Miller, R.D.** (1978) Frost heaving in non-colloidal soils. *Proceedings of the Third International Conference on Permafrost*, vol. 1, p. 708–713.
- Miller, E.E.** (1980a) Similitude and scaling of soil-water phenomena. In Chapter 12, *Applications of Soil Physics* (D. Hillel, Ed.). New York: Academic Press.
- Miller, R.D.** (1980b) Freezing phenomena in soils. In Chapter 11, *Applications of Soil Physics* (D. Hillel, Ed.). New York: Academic Press.
- Miller, R.D.** (1990) Scaling of freezing phenomena in soils. In Chapter 1, *Scaling in Soil Physics: Principles and Applications* (D. Hillel and D.E. Elrick, Ed.). Madison, Wisconsin: Soil Science Society of America.
- Miller, E.E. and R.D. Miller** (1955) Theory of capillary flow: I. Practical implications. *Soil Science Society of America Proceedings*, 19: 267–271.
- Miller, E.E. and R.D. Miller** (1956) Physical theory for capillary flow phenomena. *Journal of Applied Physics*, 27: 324–332.
- Mitchell, J.K.** (1976) *Fundamentals of Soil Behavior*. New York: John Wiley and Son.
- Nakano, Y.** (1990) Quasi-steady problems in freezing soils: 1. Analysis on the steady growth of an ice layer. *Cold Regions Science and Technology*, 17: 207–226.
- O'Neill, K. and Miller, R.D.** (1985) Exploration of a rigid ice model of frost heave. *Water Resources Research*, 21(3): 281–296.
- Pokrovsky, G.I. and I.S. Fyodorov** (1969) *Centrifuge Model Testing in the Construction Industry*. English translation from Russian by Building Research Establishment Library Translation Service.
- Savidou, C.** (1988) Centrifuge modelling of heat

transfer in soil. *Centrifuge 88* (J.-F. Corté, Ed.), p. 583–591. Rotterdam: Balkema.

**Schmidt, R.M. and K.A. Holsapple** (1980). Theory and experiments on centrifuge cratering. *Journal of Geophysical Research*, 85(B1): 235–252.

**Scott, R.F. and N.R. Morgan** (1977) Feasibility and desirability of constructing a very large centri-

fuge for geotechnical studies. Report to the National Science Foundation. Grant No. ENG 76-18871. California Institute of Technology.

**Snyder, V.A. and R.D. Miller** (1985) Tensile strength of unsaturated soils. *Soil Science Society of America Journal*, 49: 58–65.

## APPENDIX A: SOME SCALE FACTORS FOR CONVENTIONAL CENTRIFUGE MODELING

### PHYSICAL MODELING CONCEPTS

Following the presentation of Langhaar (1951), consider a physical variable of a prototype  $f_p(x_p, y_p, z_p, t_p)$  and the corresponding model quantity  $f_m(x_m, y_m, z_m, t_m)$ , where  $x, y$  and  $z$  are coordinate measures of a point within the structure,  $t$  is time, and the subscripts  $p$  and  $m$  refer to the prototype and model, respectively. The function  $f_m$  is said to be similar to the function  $f_p$  if the ratio  $f_m/f_p$  is constant for homologous points and homologous times. The constant ratio  $f = f_m/f_p$  is called the scale factor for the function  $f$ . Scale factors can be derived from model laws, i.e. ratios of physical laws for the model and prototype. When similarity is achieved, a model's response is interpreted using the scale factors to infer the response of the corresponding prototype.

The ideal for physical modeling is complete similarity, which includes geometric, kinematic, thermal and dynamic similarity. Complete similarity is usually not achieved for a model test. Scale factor conflicts and scale effects, i.e., disturbing influences that are associated with the small scale of the model, can limit similarity to a partial similarity.

When a model is made of the material of the prototype, and when there are no scale factor conflicts or disturbing scale effects, then the model material will have the same constitutive behavior as the prototype material, and prototypes with general constitutive behavior such as nonlinear elasticity and plasticity can be modeled.

### CROCE'S DERIVATION OF SCALE FACTORS FOR CONVENTIONAL GEOTECHNICAL MODELING USING SCALAR MODEL LAWS

The objective of conventional small-scale geotechnical modeling is to achieve a model response that is similar to the mechanical behavior of the prototype, and the approach is to use the prototype soil in a geometrically similar model. Thus it is important to ensure that the effective stresses in the model are the same as in the prototype at homologous points and times. The scale factors for these conditions can be derived using

scalar model laws. Closely following the analysis of Croce et al. (1985), this approach is presented here. Two assumptions are made: that soil can be treated as a continuum and that soil properties are not affected by a change in acceleration.

Dynamic similarity requires that all forces (and all kinds of forces) have the same scale factor. The forces of interest include the weight force  $F_w$ , the external force  $F_e$ , the viscous force  $F_v$ , the inertia force  $F_i$  and the seepage force  $F_s$ .

Scale factors for length  $l$ , mass  $m$  and time  $t$  are

$$K_l = \frac{l_m}{l_p}, \quad (A1)$$

$$K_m = \frac{m_m}{m_p}, \quad (A2)$$

and

$$K_t = \frac{t_m}{t_p}. \quad (A3)$$

Thus the scale factors for area  $A$  and volume  $V$  are

$$K_A = K_l^2 = \frac{A_m}{A_p} \quad (A4)$$

and

$$K_V = K_l^3 = \frac{V_m}{V_p}. \quad (A5)$$

Since the same material is used in the model and prototype at the same mass density, the scale factor for mass is equal to the scale factor for volume:

$$K_m = K_l^3 = \frac{m_m}{m_p}. \quad (A6)$$

For identical effective stresses in the model and prototype,

$$K_{\sigma'} = K_{\sigma} = K_u = \frac{\sigma'_m}{\sigma'_p} = \frac{\sigma_m}{\sigma_p} = \frac{u_m}{u_p} = 1 \quad (A7)$$

where  $\sigma'$ ,  $\sigma$  and  $u$  are, respectively, the effective stress, the total stress and the excess pore water pressure, including the capillary pressure caused by surface tension. Considering eq A4 and A7 and the definition of stress, it follows that the scale factor for all forces  $F$  should be



$$K_F = K_I^2 = \frac{F_m}{F_p} \quad (A8)$$

From the definition of *weight force*, the weight force model law and scale factor  $K_{F_w}$  is

$$K_{F_w} = \frac{F_{w_m}}{F_{w_p}} = \frac{m_m a_{g_m}}{m_p a_{g_p}} = K_I^2 \quad (A9)$$

where  $a_g$  is the acceleration due to gravity. Considering eq A6, A9 and the relation  $K_{F_w} = K_F = K_I^2$  from eq A8,

$$\frac{a_{g_m}}{a_{g_p}} = \frac{1}{K_I} \quad (A10)$$

Equation A10 implies that geotechnical modeling requires a technique that elevates the gravitational acceleration of the model.

The scale factor for an *external force*  $K_{F_e}$  must satisfy eq A8, and only technical constraints should limit this.

A *viscous force* acting on a small area  $A$  can be defined as

$$F_v = \mu_s \frac{dv}{dn} A \quad (A11)$$

where  $\mu_s$  is the viscosity of the soil skeleton and  $dv/dn$  is the velocity gradient. The model law and scale factor for the viscous force  $K_{F_v}$  can then be written

$$K_{F_v} = \frac{F_{v_m}}{F_{v_p}} = \frac{\mu_{s_m}}{\mu_{s_p}} \frac{dv_m}{dv_p} \frac{dn_p}{dn_m} \frac{A_m}{A_p} \quad (A12)$$

From the definition of velocity it follows that

$$\frac{K_I}{K_t} = \frac{v_m}{v_p} \quad (A13)$$

From eq A1, A4 and A13 and the fact that viscosity is independent of gravity,  $K_{F_v}$  can be written

$$K_{F_v} = \frac{K_I^2}{K_t} \quad (A14)$$

Because  $K_{F_v}$  must equal  $K_F = K_I^2$ , then

$$K_t = 1 \quad (A15)$$

That is, the time scale factor is 1 if the viscous force is to be scaled like the weight force.

An *inertia force* can be written as

$$F_i = ma \quad (A16)$$

where  $a$  is the acceleration. The model law and scale factor  $K_{F_i}$  for the inertia force is

$$K_{F_i} = \frac{F_{i_m}}{F_{i_p}} = \frac{m_m a_m}{m_p a_p} \quad (A17)$$

From the definition of acceleration it follows that

$$\frac{K_I}{K_t^2} = \frac{a_m}{a_p} \quad (A18)$$

From eq A6 and A18, eq A17 becomes

$$K_{F_i} = \frac{K_I^4}{K_t^2} \quad (A19)$$

Because  $K_{F_i}$  must equal  $K_F = K_I^2$ , then

$$K_t = K_I \quad (A20)$$

That is, the time scale factor is equal to the length scale factor if the inertia force is to be scaled like the weight force.

A *seepage force* can be written as

$$F_s = i W_F \quad (A21)$$

where  $W_F$  is the weight of the fluid phase and  $i$  is the hydraulic gradient defined by

$$i = \frac{v}{k} \quad (A22)$$

in which  $v$  is the superficial velocity of the fluid and  $k$  is Darcy's coefficient of permeability. From eq A21 and A22 the scale factor  $K_{F_s}$  for the seepage force can be written as

$$K_{F_s} = \frac{F_{s_m}}{F_{s_p}} = \frac{v_m}{v_p} \frac{k_p}{k_m} \frac{W_{F_m}}{W_{F_p}} \quad (A23)$$

Equation A8 implies that

$$\frac{W_{F_m}}{W_{F_p}} = K_F = K_I^2 \quad (A24)$$

Then, from eq A13 and A24, eq A23 becomes

$$K_{F_s} = \frac{K_I^3}{K_t} \frac{k_p}{k_m} \quad (A25)$$

A general expression for the coefficient of permeability is (Mitchell 1976)

$$k = \kappa \frac{\rho_w a_g}{\mu_w} \quad (\text{A26})$$

where  $\rho_w$  and  $\mu_w$  are, respectively, the density and the viscosity of the fluid phase, and  $\kappa$  is defined as the absolute permeability, which depends only on the geometry of the soil skeleton. Because  $\rho_w$ ,  $\mu_w$  and  $\kappa$  do not depend on gravity, it follows that

$$\frac{k_m}{k_p} = \frac{a_{g_m}}{a_{g_p}} = \frac{1}{K_1}. \quad (\text{A27})$$

Thus eq A25 becomes

$$K_{F_s} = \frac{K_1^4}{K_t}. \quad (\text{A28})$$

Because  $K_{F_s}$  must equal  $K_F = K_1^2$ , then

$$K_t = K_1^2. \quad (\text{A29})$$

That is, the time scale factor is equal to the length

scale factor squared if the seepage force is to be scaled like the weight force.

## CENTRIFUGE TECHNIQUE

The centrifuge is used to approximate the condition of eq A10 by subjecting a model to the constant angular velocity  $\Omega$  such that the following approximate relation holds:

$$\frac{a_{g_m}}{a_{g_p}} \approx \frac{1}{K_1} = \frac{r\Omega^2}{a_{g_p}} \quad (\text{A30})$$

where  $a_{g_p}$  is the acceleration due to Earth's gravity,  $r$  is a representative radius of the model from the axis of rotation (Cooke 1991), and  $r\Omega^2$  is the radial centripetal acceleration of the model at this radius. In the centrifuge modeling literature,  $N$  or  $n$  is often used as the symbol for the inverse of the length scale factor, i.e.,  $1/K_1$ .

## APPENDIX B: SCALING THE RIGIDICE MODEL

The Rigidice model of frost heave is a set of differential equations expressing mass, energy and force balances in the frozen fringe for air-free, colloid-free and solute-free soil (Miller 1978). A set of reduced or scaled variables for this model were later presented by Miller (1990). To avoid redundancy, this later work did not contain derivations but referred to the earlier classic works for ice-free unsaturated soil (Miller and Miller 1955, Miller 1980a). For completeness of this paper, this appendix presents a brief derivation of the reduced variables presented by Miller for the liquid water and solid ice phases. It also serves as an example of how the seemingly subjective process of scaling equations is performed. All scaled variables will be given upper-case letters to distinguish them from the nonscaled dimensional variables that are in lower case.

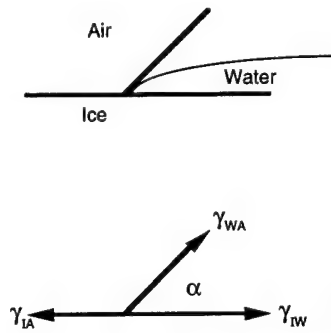


Figure B1. Equilibrium configuration.

We start with Young's equation relating the contact angle  $\alpha$  and the surface tensions for all three phases of water:

$$\gamma_{IA} = \gamma_{IW} + \gamma_{WA} \cos \alpha \quad (B1)$$

in which  $\gamma$  is the surface tension and the subscripts I, W and A are for ice, water and air, respectively. Figure B1 is a schematic of the equilibrium configuration and force diagram about the point of mutual contact for all three interfaces. Since  $\cos \alpha$  is already dimensionless, eq B1 can only be made dimensionless by dividing through by one of the surface tensions. A reasonable choice is  $\gamma_{IA}$  with the largest magnitude, which results in the reduced Young's equation

$$1 = \Gamma_{IW} + \Gamma_{WA} \cos \alpha \quad (B2)$$

where the reduced surface tensions are

$$\Gamma_{IW} \equiv \frac{1}{\gamma_{IA}} \gamma_{IW} \quad (B3)$$

and

$$\Gamma_{AW} \equiv \frac{1}{\gamma_{IA}} \gamma_{AW} .$$

To simplify, the remainder of this appendix will address ice-water systems. A similar set of equations for water-air and ice-air systems are obtained by direct analogy to the ice-water equation and are listed by Miller (1990).

The distinguishing trait exhibited by water and ice in a porous medium that does not exist in unrestricted bulk is the existence of curved interfaces. The force balance across a curved interface separating two phases in equilibrium is given by the Laplace surface tension equation, which for an ice-water interface is

$$p_I - p_W = 2 \frac{\gamma_{IW}}{r_{IW}} \quad (B4)$$

where the absolute pressure is  $p$  (N/m<sup>2</sup>) and the mean radius of curvature is  $r$ . In the case of frozen soil, this equation expresses the behavior of water and ice contained within the pores. This suggests a length scale on the order of the pore size, so we introduce a microscopic length  $\lambda$ . Equation B4 contains three variables,  $p_I$ ,  $p_W$  and  $r$ , and one constant,  $\gamma_{IW}$ . Equation B3 shows how to reduce the surface tension. At this point we need to decide how to reduce the remaining variables. The simplest approach is to acknowledge that the radius of curvature is a pore length dimension, so it is reduced by dividing by  $\lambda$ . The reduced curvature is therefore

$$R_{IW} \equiv \frac{1}{\lambda} r_{IW} . \quad (B5)$$

Substituting B3 and B5 into the right hand side of B4 determines the reduced pressure by dimensional equivalence:

$$P \equiv \frac{\lambda}{\gamma_{IA}} p \quad (B6)$$

giving the reduced form of the Laplace surface tension equation:

$$P_I - P_W = 2 \frac{\Gamma_{IW}}{R_{IW}} . \quad (B7)$$

At thermodynamic equilibrium the chemical potentials of ice and water are equal and are ex-

pressed by the differential form of the Gibb's relationship. It has been shown (Loch 1978, Black 1992) that the Gibb's relationship for monocomponent and multicomponent systems contained within a porous medium that subjects the water to a general body force can be expressed in a simplified Clapeyron equation. When pressures are given in standard gauge pressures  $u$ , the Clapeyron equation is written as

$$u_W - \frac{u_I}{\gamma_{IW}} = \frac{h_{IW}}{\theta_o} \theta \quad (B8)$$

in which  $h_{IW}$  is the volumetric latent heat of fusion ( $\text{J/m}^3$ ),  $\gamma_{IW}$  is the specific gravity of ice and  $\theta$  ( $^{\circ}\text{C}$ ) is the elevation of the melting point of ice from the standard melting point of ice  $\theta_o$ . For normal water,  $\theta$  will be negative.

The gauge pressures will scale the same as the absolute pressures:

$$U \equiv \frac{\lambda}{\gamma_{IA}} u. \quad (B9)$$

The specific gravity of ice is already dimensionless, so the remaining constants  $\theta_o$  and  $h_{IW}$  must be used to reduced the only variable: temperature  $\theta$ . Earlier scaling attempts by Miller (Black 1985) developed a reduced temperature that included the latent heat term, but for the benefit of clarity, Miller (1990) suggested a different reduced temperature:

$$\Theta \equiv \frac{1}{\theta_o} \theta. \quad (B10)$$

Substituting these scaling parameters for pressure and temperature into eq B8 results in an additional reduced term called the reduced latent heat:

$$H_{IW} \equiv \frac{\lambda}{\gamma_{IA}} h_{IW}. \quad (B11)$$

These scaling relationships give a reduced Clapeyron equation:

$$U_W - \frac{U_I}{\gamma_{IW}} = H_{IW} \Theta. \quad (B12)$$

The Laplace and Clapeyron equations show that the pressures, temperature and curvature are interrelated. When the porous medium is geometrically complicated, as in the case of soil, it is helpful to simplify the pressures-curvature behavior by expressing the Laplace equation with empirically determined material properties. In our case the necessary material properties are the volume fractions for water  $W(u_W, u_I)$ , ice  $I(u_W, u_I)$

and grains  $G$ . These volume fractions are related by

$$G + W(u_W, u_I) + I(u_W, u_I) = 1. \quad (B13)$$

The complete scaled form is simply

$$G + W(U_W, U_I) + I(U_W, U_I) = 1. \quad (B14)$$

The criterion for lens initiation is obtained from the geotechnical concept of effective stress, or the particle-to-particle contact stress. When this stress is zero, the particles no longer remain in contact and an ice lens is able to form. The Snyder-Terzaghi equation partitions the total confining stress  $\sigma_T$  ( $\text{N/m}^2$ ) between the effective  $\sigma_e$  ( $\text{N/m}^2$ ) and neutral or pore  $\sigma_n$  ( $\text{N/m}^2$ ) stresses at locations near the initiation of an ice lens:

$$\sigma_T = \sigma_e + \sigma_n. \quad (B15)$$

Figure B2 shows the partitioning of these stresses. The effective and neutral stresses in this relationship are different from the traditional stresses in the Terzaghi equation because these include Snyder's flawed solid theory (Snyder and Miller 1985). These stresses, like the pressure, take place at the pore scale, so they will scale just as pressures do:

$$\Sigma = \frac{\lambda}{\gamma_{IA}} \sigma. \quad (B16)$$

The flow of water through the frozen fringe is assumed to obey Darcy's law:

$$v_W = k_W(u_W, u_I)(f_W - \nabla u_W) \quad (B17)$$

in which  $v_W$  is the volumetric flux of water ( $\text{m}^3/\text{m}^2\text{s}$ ),  $k_W(u_W, u_I)$  is the capillary conductivity ( $\text{m}^4/\text{Ns}$ ),  $f_W$  is the body force per unit volume ( $\text{N/m}^3$ ) and  $\nabla$  is the gradient. To reduce Darcy's law we begin by examining the last term. This is the gradient of water pressure across the region of interest. If we are looking at flow through an individual pore, then this length would appear to be  $\lambda$ . This would be correct for this special and very limited case. In general, far more complex flow patterns through a myriad of pore geometries containing different amounts of ice and

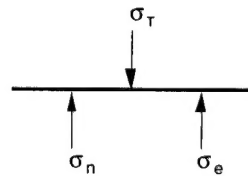


Figure B2. Stress partitioning of ice, water and air.

water are of concern. At this scale we refer to the porous medium behaving as a continuum displaying uniform material properties, and we are interested in the flow into and then out of a volume of material. This suggests that a different length scale is required to describe the gradient, since  $\lambda$  is applicable only at the pore scale. The additional macroscopic length scale is  $\zeta$ . Using this new length scale to reduce the gradient operator results in the reduced body force:

$$F_W \equiv \frac{\zeta \lambda}{\gamma_{AW}} f_W. \quad (B18)$$

The proportionality factor in Darcy's equation is the source of much confusion. In eq B17 it is expressed as capillary conductivity  $k_W$ . Soil scientists tend to use hydraulic conductivity  $K$  (m/s), and geologists and petroleum engineers use intrinsic permeability  $k$  (m<sup>2</sup>). These three parameters are related by

$$k_W = \frac{K}{\rho g} = \frac{k}{\eta} \quad (B19)$$

in which  $\rho$  (kg/m<sup>3</sup>) is the density of water,  $g$  is the acceleration due to gravity (or other body force) and  $\eta$  (N/m<sup>2</sup>s) is the viscosity of water. They are all functions of water and ice content, which are functions of the water and ice pressures.

The process of scaling the capillary conductivity consists of first realizing that it is already inversely proportional to viscosity (i.e., eq B19), so it must therefore be scaled by multiplying by the viscosity. It then becomes the intrinsic permeability, which is in dimensions of length squared. To complete the scaling we must decide on the correct length scale to use. Again relying on the continuum approximation, the conductivity should not depend on the size of the sample once it attains the minimum size required for the continuum approximation. This requires the use of the microscopic length scale  $\lambda$  to scale the conductivity. Miller and Miller (1955) deduced the same length scale choice by considering the Navier-Stokes equation applied to flow through the pore. The reduced capillary conductivity is then

$$K_W \equiv \frac{\eta}{\lambda^2} k_W. \quad (B20)$$

Substituting eq B20, B19, B6 and the scaling factor  $\zeta$  to reduce the gradient operator into eq B17 gives the scaled form of Darcy's equation:

$$V_W = K_W (U_I, U_W) (F_W - \nabla U_W) \quad (B21)$$

in which the reduced volumetric flux of water  $V_W$  is, by balancing constants,

$$V_W \equiv \frac{\zeta \eta}{\lambda \gamma_{IA}} v_W. \quad (B22)$$

The continuity equation for pore constituents is

$$\begin{aligned} \nabla \bullet (v_W + Y_{IW} v_I) \\ = - \frac{\partial}{\partial t} [W(u_W, u_I) + Y_{IW} I(u_W, u_I)] \end{aligned} \quad (B23)$$

in which  $v_I$  (m<sup>3</sup>/m<sup>2</sup>s) is the volumetric flux of ice and  $t$  is time. The operator  $\nabla \bullet$  is the divergence, which simply scales by multiplying by  $\zeta$ . The volumetric flux of ice must scale like the volumetric flux of water to maintain dimensional equality on the left side of eq B23. Since the volumetric water and ice contents are already dimensionless, the reduced time  $T$  is

$$T \equiv \frac{\lambda \gamma_{IA}}{\zeta^2 \eta} t. \quad (B24)$$

The conservation of thermal energy is

$$\begin{aligned} \nabla \bullet (v_H + h_{IW} v_W) = - \frac{\partial}{\partial t} [C_H(u_W, u_I) \theta \\ + h_{IW} W(u_W, u_I)] \end{aligned} \quad (B25)$$

in which  $v_H$  (W/m<sup>2</sup>) is the macroscopic flux of sensible heat and  $C_H(u_W, u_I)$  (J/m<sup>3</sup> K) is the volumetric heat capacity excluding heat resulting from phase change. The volumetric heat capacity is assumed to be a material property that is constant in the continuum assumption for a given state of ice and water contents. Starting with the left side of eq B25 the reduced macroscopic flux of sensible heat  $V_H$  is obtained

$$V_H \equiv \frac{\zeta \eta}{\gamma_{IA}^2} v_H. \quad (B26)$$

The reduced volumetric heat capacity  $C_H$  must therefore be

$$C_H(U_W, U_I) \equiv \frac{\lambda \theta_0}{\gamma_{IA}} C_H(u_W, u_I). \quad (B27)$$

The macroscopic flux of sensible heat is given by Fourier's law:

$$V_H = -k_H(u_W, u_I) \nabla \theta \quad (\text{B28})$$

in which  $k_H$  (W/mK) is the thermal conductivity. This conductivity is also a material property that is assumed to be constant in the continuum sense for a given state of water and ice contents. The reduced thermal conductivity is then

$$K_H(U_W, U_I) \equiv \frac{\eta \theta_o}{\gamma_{IA}^2} k_H(u_W, u_I). \quad (\text{B29})$$

The most important characteristic of the Rigidice model that sets it apart from others is the concept of thermally induced regelation. This results in the inclusion of an extra mass flux resulting from the bulk movement of ice in the frozen fringe. The velocity of ice movement in the fringe is the heave velocity  $v_R$  (m/s) relative to the stationary grains of the porous media below the fringe. The volumetric flux of ice  $v_I$  (m<sup>3</sup>/m<sup>2</sup>s) resulting from this regelation is

$$v_I = I(u_W, u_I) v_R. \quad (\text{B30})$$

From eq B22 we know how volumetric fluxes scale, so the reduced regelation velocity is therefore

$$V_R \equiv \frac{\zeta \eta}{\lambda \gamma_{IA}}. \quad (\text{B31})$$

This completes the scaling of the more important variables and parameters involved in ground freezing. A list of all scaled variables applicable to ground freezing, as well as all water phases, was presented by Miller (1990).

An example of how heaving experiments should be interpreted by reduced variables seems in order. Given two experiments using the same soil

but subjected to different body forces, eq B18, B10 and B24 show how they must relate. Using the convention of calling the laboratory reference experiment the prototype  $p$  and the experiment subjected to the different body force  $m$  for model, the reduced body force  $F_W$  must be equal for both:

$$\frac{\zeta_p \lambda_p}{\gamma_{IA}} f_p = \frac{\zeta_m \lambda_m}{\gamma_{IA}} f_m. \quad (\text{B32})$$

If we say that  $f_m = 100 f_p$ , as might be expected in a centrifuge, and we use the same soil in both experiments, then the total lengths of the two experiments are related by  $\zeta_m = 0.01 \zeta_p$ . Since the reduced temperatures  $\Theta$  must be equal at corresponding locations, the actual temperatures  $\theta$  will therefore be the same in both the prototype and the model. This leads to the most important experimental consequence of centrifuge modeling. Since the reduced times  $T$  must be equal, the actual times are related by  $t_m = t_p / 100^2$ . Scaled experiments are finished in a very timely manner compared to similar laboratory experiments.

A final note is on the meaning of the microscopic length  $\lambda$ . If the porous medium consisted of identical pores, then this length would just be the pore size. But in real porous media there is a distribution of sizes and geometries of pores. The microscopic length in these cases represents some averaged value of the pores. It is more like the size of the smallest representative elementary volume (REV) that begins to describe the porous media as a continuum of uniform material properties. The difficulty is in actually measuring this parameter without completely destroying the original material.

# REPORT DOCUMENTATION PAGE

Form Approved  
OMB No. 0704-0188

Public reporting burden for this collection of information is estimated to average 1 hour per response, including the time for reviewing instructions, searching existing data sources, gathering and maintaining the data needed, and completing and reviewing the collection of information. Send comments regarding this burden estimate or any other aspect of this collection of information, including suggestion for reducing this burden, to Washington Headquarters Services, Directorate for Information Operations and Reports, 1215 Jefferson Davis Highway, Suite 1204, Arlington, VA 22202-4302, and to the Office of Management and Budget, Paperwork Reduction Project (0704-0188), Washington, DC 20503.

|   |   |   |                                      |
|---|---|---|--------------------------------------|
| 1. AGENCY USE ONLY (Leave blank)  | 2. REPORT DATE<br>May 1995                                  | 3. REPORT TYPE AND DATES COVERED  |                                      |
| 4. TITLE AND SUBTITLE<br><br>Initial Results From Small-Scale Frost Heave Experiments in a Centrifuge   |   | 5. FUNDING NUMBERS<br><br>ILIR and<br><br>PE: 6.27.84A<br>PR: 4A762784AT42<br>TA: CA<br>WU: D02 |                                      |
| 6. AUTHORS<br><br>Stephen A. Ketcham and Patrick B. Black   |   |   |                                      |
| 7. PERFORMING ORGANIZATION NAME(S) AND ADDRESS(ES)<br><br>U.S. Army Cold Regions Research and Engineering Laboratory<br>72 Lyme Road<br>Hanover, New Hampshire 03755-1290   |   | 8. PERFORMING ORGANIZATION<br>REPORT NUMBER<br><br>CRREL Report 95-9                            |                                      |
| 9. SPONSORING/MONITORING AGENCY NAME(S) AND ADDRESS(ES)<br><br>Office of the Chief of Engineers<br>Washington, D.C. 20314-1000  |   | 10. SPONSORING/MONITORING<br>AGENCY REPORT NUMBER   |                                      |
| 11. SUPPLEMENTARY NOTES   |   |   |                                      |
| 12a. DISTRIBUTION/AVAILABILITY STATEMENT<br><br>Approved for public release; distribution is unlimited.<br><br>Available from NTIS, Springfield, Virginia 22161   |   | 12b. DISTRIBUTION CODE  |                                      |
| 13. ABSTRACT (Maximum 200 words)<br><br>Frost heave modeling is presented as a problem of small-scale experimental modeling. Scale factors applicable to frost heave model testing are reviewed, and initial data from frost heave experiments conducted as centrifuge model tests are presented. Ongoing improvements, modifications and future model tests are discussed. |   |   |                                      |
| 14. SUBJECT TERMS<br><br>Frost heave                      Modeling  |   | 15. NUMBER OF PAGES<br>23   |                                      |
|   |   | 16. PRICE CODE  |                                      |
| 17. SECURITY CLASSIFICATION<br>OF REPORT<br>UNCLASSIFIED  | 18. SECURITY CLASSIFICATION<br>OF THIS PAGE<br>UNCLASSIFIED | 19. SECURITY CLASSIFICATION<br>OF ABSTRACT<br>UNCLASSIFIED                                      | 20. LIMITATION OF ABSTRACT<br><br>UL |